JOURNAL OF GEOPHYSICAL RESEARCH, VOL. 87, NO. C8, PAGES 5667–5680, JULY 20, 1982

The Variation of Sea Surface Temperature in 1976 and 1977 1: The Data Analysis

K. MIYAKODA AND A. ROSATI

Geophysical Fluid Dynamics Laboratory/NOAA, Princeton University, Princeton, New Jersey 08540

To study the spatial distribution of the sea surface temperature (SST) for the years of 1976 and 1977, ship and satellite data at 1° quadrangles were collected. Two points were investigated: (1) the difference of monthly mean SST data between the two sources, and (2) map analyses over the globe. The study shows that without satellite data, an adequate coverage of world ocean is not possible and that there is a large difference in values between the ship and satellite data. The standard deviation of the difference between the satellite and merchant ship SST data for monthly and 1° quadrangle mean was ±1.49°C, where the sampling errors were not subtracted. Using these data, analyses were created and compared with independent analyses. The comparisons included large-scale analyses and two small-scale analyses. Attention was focussed specially on (1) the utility of the satellite SST data and (2) the data quality control. The large-scale analyses agreed well with the independent analyses. However, both of the small-scale analyses did not compare well.

1. INTRODUCTION

The winter of 1976–1977 was the coldest on record for the midwestern United States, particularly in the Ohio Valley, where averaged monthly mean atmospheric temperatures were more than 8°C (or 11°C) lower than the normal [see, for example, *Diaz and Quayle,* 1978; *Wagner,* 1977]. As has been speculated by *Namias* [1978] and others, this anomalous atmospheric phenomenon is likely to be related to the ocean temperature particularly over the North Pacific. Namias pointed out that 'North Pacific sea-surface temperatures (SST's) during the summer of 1976 had reached all time lows since 1947,' as is shown by Figure 1. Interestingly, another anomalously severe winter again attacked the eastern United States in 1978; particularly cold months were February and March 1978.

The objective of this paper is to investigate the variation of SST on a global basis throughout the years 1976 and 1977. In these years, the SST data of the NOAA-5 satellite and the techniques of the data processing have finally reached a level of accuracy that one can consider, for the first time, deriving world-ocean maps of SST [*Strong and Pritchard,* 1980].

In part 1, map analyses of SST will be presented. We have noticed that there are other laboratories and centers that produce synoptic maps of SST. In particular, U.S. Navy Fleet Numerical Weather Central (FNWC), Monterey, California, and Scripps Institution of Oceanography (SIO), La Jolla, California, both of which used ship data only; National Environmental Satellite Service (NESS), NOAA, Washington, D.C., which used satellite data only; and National Meteorological Center (NMC), NOAA, Washington, D.C., which used both ship and satellite data [*Gemmill and Larson,* 1979]. Our maps will be compared with those.

2. LEVEL II DATA COVERAGE

The terminology 'Level II data' was introduced by the Joint GARP (Global Atmospheric Research Program) Organizing Committee to specify the digitized values processed from raw observations. Sometimes processing means the conversion from measurement variables to conventional parameters, or it could mean thinning data by spatial or temporal averaging or filtering, and other times it could mean an appropriate validation. The satellite SST data, after having been processed from raw retrievals (level I data) are an example of level II data. The processed SST data of merchant vessels are other examples of level II data.

For this study we have used level II ship data supplied by Douglas R. McLain, National Marine Fisheries Service, Monterey, California. The data are monthly means on 1° quadrangles and have undergone quality control. The satellite level II data were taken from NESS SST archive tapes. These data were processed by the histogram method, a detailed and recent procedure was described by *Brower et al.* [1976].

Examples of ship and satellite data coverage are displayed in Figures 2 and 3. In both figures, the asterisks (the larger dots) represent the locations, at which five or more observations were available within the 1° quadrangle, and the small dots represent the locations of less than five observations. As is seen, the distribution of ship data reflects shipping lanes connecting major seaports. On the other hand, the distribution of satellite data reflects weather activity; e.g., the mid-latitude clouds and the ITCZ (inter-tropical convergence zone) clouds are clearly discernible. This difference in the distribution of the data sets is often complementary.

An example of this would be in the region of the Gulf Stream and the Kuroshio Current, where ship data are plentiful, and satellite data, due to cloud cover during winter months, are quite sparse. Over the southern hemisphere, however, we find adequate satellite coverage (Figure 3) but inadequate ship coverage (Figure 2) due to relatively few ship observations. For both ship and satellite, monthly means were computed by taking all the observations (level II data), within a 1° quadrangle, and averaging them for a particular month. Over the world ocean the total number of 1° quadrangles are 42311 (it should be noted that this number includes quadrangles that contain ice). For January 1978 the number of 1° quadrangles containing monthly means was 11953 for ship data and 25052 for satellite data. It must be, however, remembered that looking only at the amount of data does not provide the whole picture of the data coverage. The satellite data are rather homogeneously distributed, whereas the ship data are nonuniformly distributed.

Paper number 2C0620.

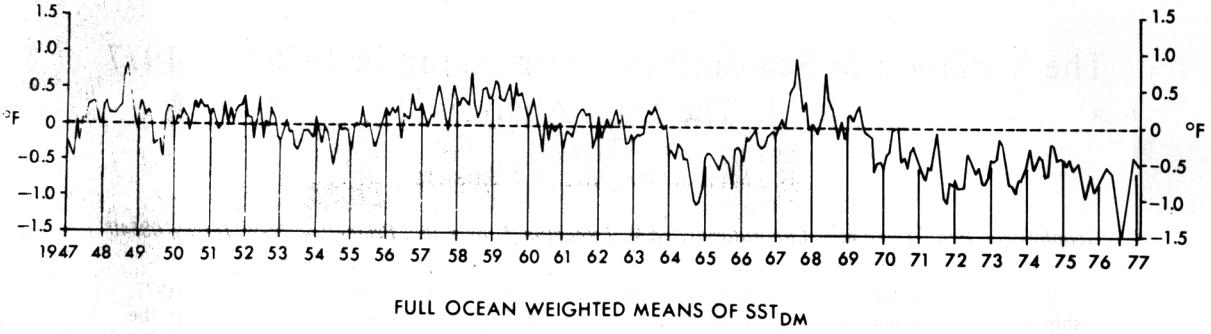

Fig. 1. Monthly mean SST anomalies (°F) averaged over the Pacific Ocean north of 20°N from 1947 through January 1977. Horizontal broken line is the mean for the 20-year period, 1947–1966 [*Namias*, 1978].

These numbers and the data distributions do not vary appreciably from month to month throughout 1976 and 1977. It is certain that monthly mean ship or satellite data alone cannot cover the world oceans, and, presently, even the satellite-ship composite observing system is inadequate for 10-day means. However, using the 1979 FGGE (First GARP Global Experiment) data, which used the TIROS-N and NOAA-A polar orbiting satellites, more frequent map analysis may be produced.

3. Accuracies of Level II Data

Evaluation of the quality of SST data has been conducted by a number of investigators. Most of the information was, however, documented only in technical notes or internal office notes. The data from merchant ships were compared with those of research ships or time series from ocean stations as the ground truth. Four types of SST measurement frequently used are bathythermograph temperatures deployed by research ships or aircraft, bucket temperatures, engine-intake temperatures made by commercial or weather ships, and satellite-derived temperatures.

Saur's [1963] study based on a sample of 12 ships in the Pacific Ocean revealed that the mean difference between bucket temperature and intake temperature was 0.67°C and that the standard deviation was ±0.89°C for SST data. A more recent study of *Tabata* [1978*a*] made at ocean station Papa and eight NOAA buoy stations in the Northern Pacific Ocean compared temperature obtained at these stations with merchant ships in their vicinities and found that the ships' temperatures are on the average 0.2 ± 1.5°C greater than those of the stations. It must be remembered that in their study the SST's reported by the ships are those taken directly from the meteorological teletype circuit and therefore were not quality controlled to exclude possible erroneous values, and they may have influenced the estimate made.

Since the first global coverage of satellite SST remote sensing by ITOS-1 in 1970, the accuracy of the satellite-derived SST has been investigated by several groups [*Rao et al.*, 1972; *Brower et al.*, 1976]. Ships' data are currently being used as ground truth for satellite observations, although ship and satellite data are fundamentally of a different nature. It is understood that the basic difference originates from the difference between a subsurface measurement versus an areal measurement. Ship measurements are usually made at 3–6 m below the water line, while satellite values

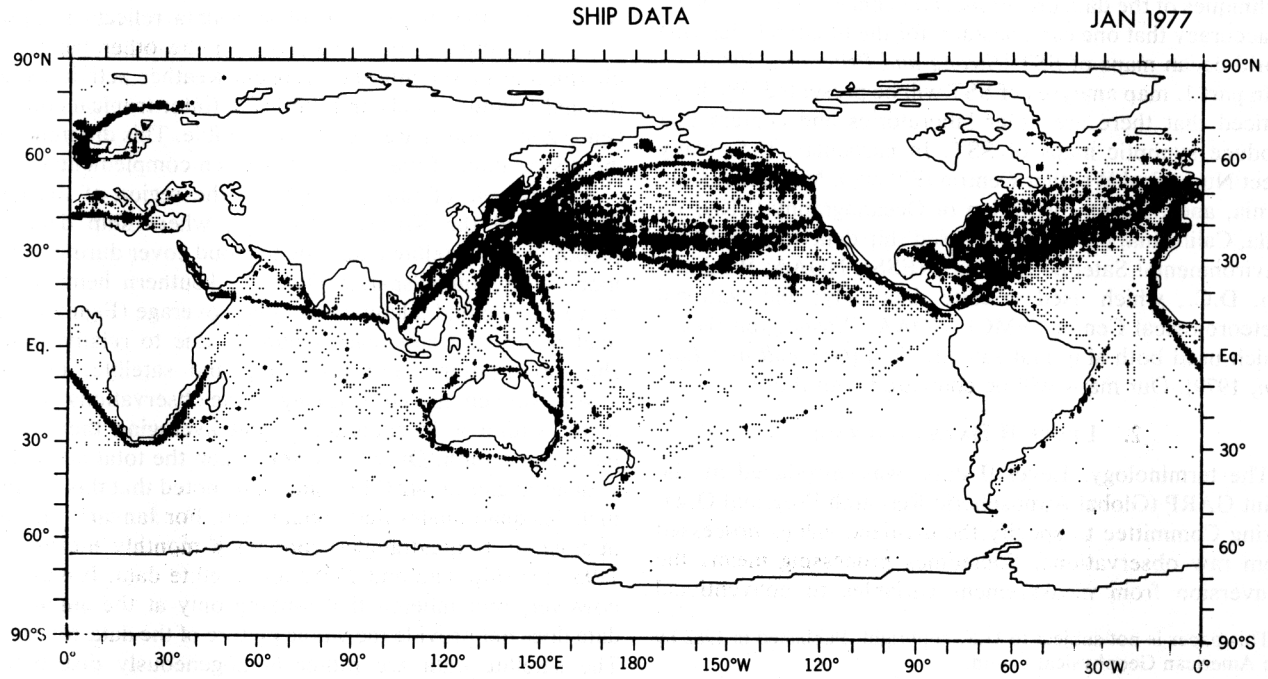

Fig. 2. The ship data available for January 1977.

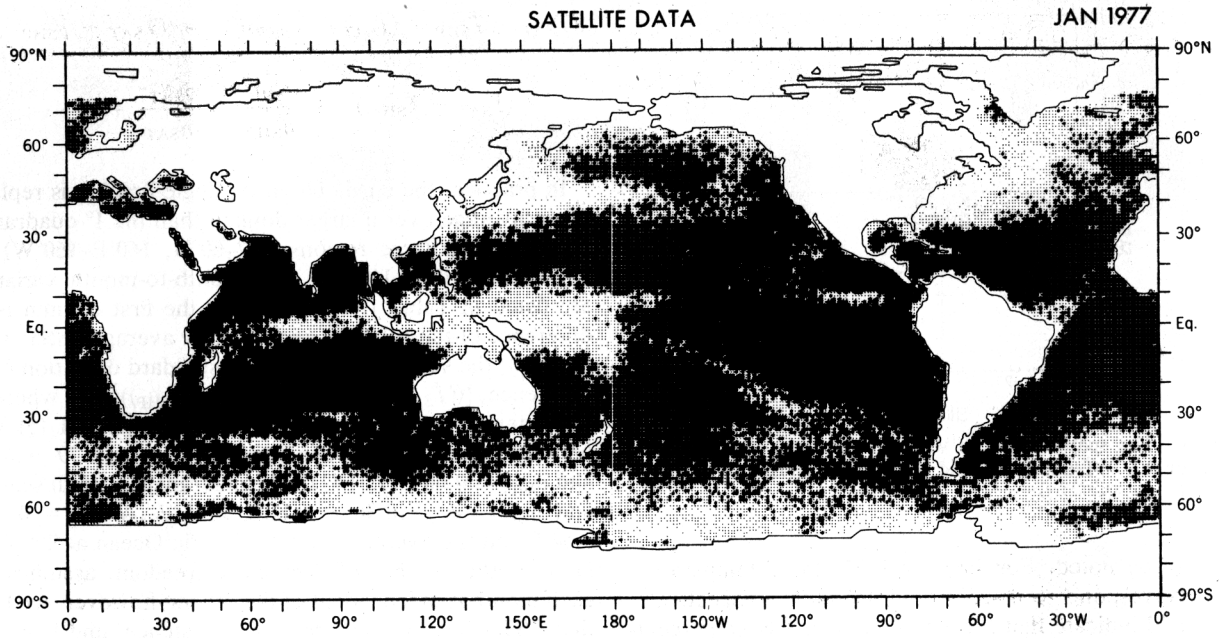

Fig. 3. The satellite data available for January 1977.

are 'skin temperatures' supposedly for the upper millimeter of the ocean surface. The satellite SST is inadvertently an area average, whereas the ship SST is a point value. In terms of distribution of measurements, satellite observations are quite good. They exhibit less variance than ship 'intake' temperature over a region, and this means they are more desirable for our purpose of an atmospheric impact study. However, satellite SST's simultaneously may reveal systematic biases, e.g., incorrect atmospheric attenuation for local meteorological conditions [*Brower et al.*, 1976]. According to *Walton et al.* [1976], recent satellite data processing has had a significant improvement in cloud detection and atmospheric attenuation correction, using multi-channels of the radiometers.

Satellite soundings can sense the subtle spatial structure of the temperature field; this fact has often been pointed out for the visible and infrared imagery of the sea surface [*Stump and Legeckis*, 1977; *Legeckis*, 1978]. *Barnett et al.* [1979] found that for the central tropical Pacific that satellite SST products were biased by 1°–4°C and were not useful by themselves. According to R. L. Brower (personal communication, 1979), the satellite retrievals are still in the development stage, and the quality of the data has changed due to the retrieval technique.

We also compared satellite and merchant ship data, but unlike previous studies, which restricted themselves to a limited region and a short time period, we created monthly mean data at 1° quadrangles over the globe, wherever data are available. Figures 4 and 5 are examples of this comparison. The plot was made whenever a paired observation from the two sources was available within the same 1° quadrangle. Normally, the largest errors in ship report are produced by faulty radio transmission and by incorrect reporting or receiving of ships' position. In our case, a preliminary quality control was done by McLain and then another screening was applied by tossing out data that when compared with the monthly climatological normals exceeded 5°C. This value of 5°C was arbitrarily chosen as a cutoff criteria between 'realistic' and 'unrealistic' values.

At a glance of Figures 4 and 5, the correspondence appears to be good. However, upon looking at Figure 4, we see that between 295° and 300°K and between 275° and 280°K a systematic bias toward satellite data being colder than ship

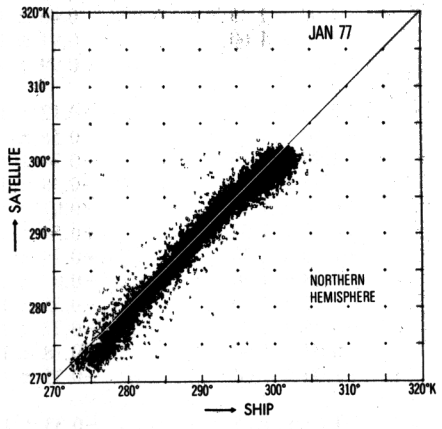

Fig. 4. The scatter diagram of the satellite versus the ship total SST data over the northern hemisphere for January 1977.

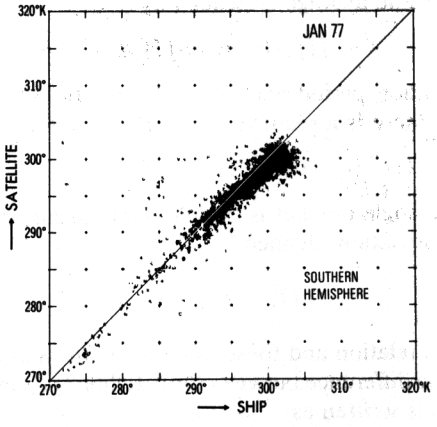

Fig. 5. The same as in Figure 4 but over the southern hemisphere.

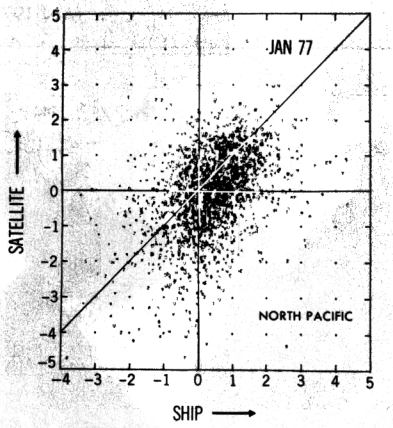

Fig. 6. The scatter diagram which is the same as in Figure 4 except for the SST anomalies and for the domain of 160°E–160°W, 20°–60°N.

data may be noted. For January 1977, these temperature ranges correspond to 0°–25°N and 45°–60°N, respectively. This would indicate that areas that contain a large percentage of cloud cover would yield satellite SST's that tend to be too cool. *Barnett et al.* [1979] also noted the same bias in the tropical Pacific and stated that the majority of the error is proportional to the cloud cover and water vapor content in the lower atmosphere. Our interest is in the anomaly of SST, that is the departure from normal. Figure 6 is a scatter diagram of the SST anomalies for the same case as that in Figure 4; the anomalies for both ship and satellite data are the deviations from the RAND normal [*Alexander and Mobley*, 1976]. For this figure we required that there be five or more satellite observation and three or more ship observation within each 1° quadrangle. The agreement between the satellite and ship data are not good and the same bias, as noted previously, exists (i.e., the satellite data overall seem colder).

A statistical study was undertaken to look at the differences between the two types of data in the North Pacific, over all months of 1976 and 1977. We used the monthly mean SST averaged over 1° quadrangles. In practice, however, the average is performed over a finite number of observations, n, for a 1-month period and within a 1° quadrangle, i.e.,

$$\bar{T} = \sum_{i=1}^{n} T_i/n \tag{1}$$

where the true average is defined by

$$\bar{T} = \iiint T\,dx\,dy\,dt / \iiint dx\,dy\,dt \tag{2}$$

the integration period and domain being the same. In this situation, there is a relation between $\bar{T}$ and $\bar{T}$ as

$$\langle(\bar{T} - \bar{T})^2\rangle = \sigma^2/n \tag{3}$$

where the angle bracket is the ensemble mean and σ is the standard deviation, defined by

$$[\langle(T_i - \bar{T})^2\rangle]^{1/2} = \sigma \tag{4}$$

Using this relation and these definitions, the standard deviation of the difference between the satellite $\bar{T}_{SAT}$ and the ship data $\bar{T}_{SHP}$ is written as

$$\langle(\bar{T}_{SAT} - \bar{T}_{SHP} - \langle\bar{T}_{SAT} - \bar{T}_{SHP}\rangle)^2\rangle = \langle(\bar{T}_{SAT} - \bar{T}_{SHP} - \langle\bar{T}_{SAT} - \bar{T}_{SHP}\rangle)^2\rangle + \frac{\sigma_{SHP}^2}{n_{SHP}} + \frac{\sigma_{SAT}^2}{n_{SAT}} + \cdots \tag{5}$$

In practice, the ensemble mean angle bracket is replaced by an average over a larger domain than the 1° quadrangle. We took two large regions (40°–60°N, 160°E–160°W) and (20°–40°N, 140°E–160°W). The month-to-month variations are listed in Table 1. In this table, the first column is the difference of the spatially and monthly averaged SST, $\langle\bar{T}_{SAT} - \bar{T}_{SHP}\rangle$; the second column is the standard deviation of the difference, $[\langle(\bar{T}_{SAT} - \bar{T}_{SHP} - \langle\bar{T}_{SAT} - \bar{T}_{SHP}\rangle)^2\rangle]^{1/2}$; where the extra terms on the right-hand side in equation (5) were omitted. According to our survey, $\sigma_{SHP} = 0.79 \sim 1.9$°C and $\sigma_{SAT} = 0.68 \sim 1.21$°C for 1° quadrangle over all seasons, and $\sigma_{SHP}/\sqrt{n} = 0.36 \sim 0.80$°C and $\sigma_{SAT}/\sqrt{n} = 0.33 \sim 0.54$°C, on the average over the Pacific Ocean at 20°–60°N. Here n, the number of degrees of freedom, assumes that each month is independent of the others; however, we know that SST's have a great deal of persistence, and hence the sampling error range shown here could be larger. Looking at the first column, the mean difference, we see that negative values dominate at the middle latitudes, 40°–60°N, implying that satellite temperatures are lower than ship temperatures, again probably due to cloud contaminated retrievals. On the other hand, in the lower latitudes, 20°–40°N, the differences are more positive particularly during summer months. The standard deviation ranges from ±1.18° to ±2.3°C, ±1.49°C being the arithmetic average for the entire period and domain. Overall, however, it is difficult to make a simple, clear cut statement on the characteristic of the seasonal variation.

TABLE 1. $(\bar{T}_{SAT} - \bar{T}_{SHP})$ ± Standard Deviation

	Middle Latitude, 40°–60°N, 160°E–160°W	Lower Latitude, 20°–40°N, 160°E–160°W
1976		
Jan.	−1.85 ± 1.35	0.84 ± 1.47
Feb.	−1.75 ± 1.55	0.04 ± 1.17
March	−1.30 ± 1.25	0.19 ± 1.17
April	−1.20 ± 1.20	0.79 ± 1.40
May	−0.97 ± 1.50	0.94 ± 1.20
June	−1.19 ± 1.85	1.22 ± 1.30
July	−0.08 ± 1.50	1.01 ± 1.43
Aug.	−0.35 ± 1.80	0.07 ± 1.18
Sept.	−0.71 ± 1.45	−0.58 ± 1.25
Oct.	−1.00 ± 1.35	0.46 ± 1.31
Nov.	−1.40 ± 1.60	0.91 ± 1.49
Dec.	−1.08 ± 1.50	0.99 ± 1.23
1977		
Jan.	−2.10 ± 1.45	+0.12 ± 1.23
Feb.	−2.50 ± 1.30	−0.56 ± 1.27
March	−1.90 ± 1.40	−0.34 ± 1.33
April	−1.95 ± 1.95	−0.38 ± 1.53
May	−0.58 ± 1.75	−0.07 ± 1.43
June	+0.38 ± 2.05	+0.54 ± 1.83
July	+2.70 ± 2.30	+0.74 ± 1.77
Aug.	+0.38 ± 1.70	−0.6 ± 1.33
Sept.	−0.32 ± 1.50	−0.55 ± 1.27
Oct.	−0.95 ± 1.90	−0.27 ± 1.43
Nov.	−0.67 ± 1.80	+0.18 ± 1.43
Dec.	−1.00 ± 1.60	+0.35 ± 1.5
1978		
Jan.	−1.65 ± 1.55	−0.33 ± 1.3

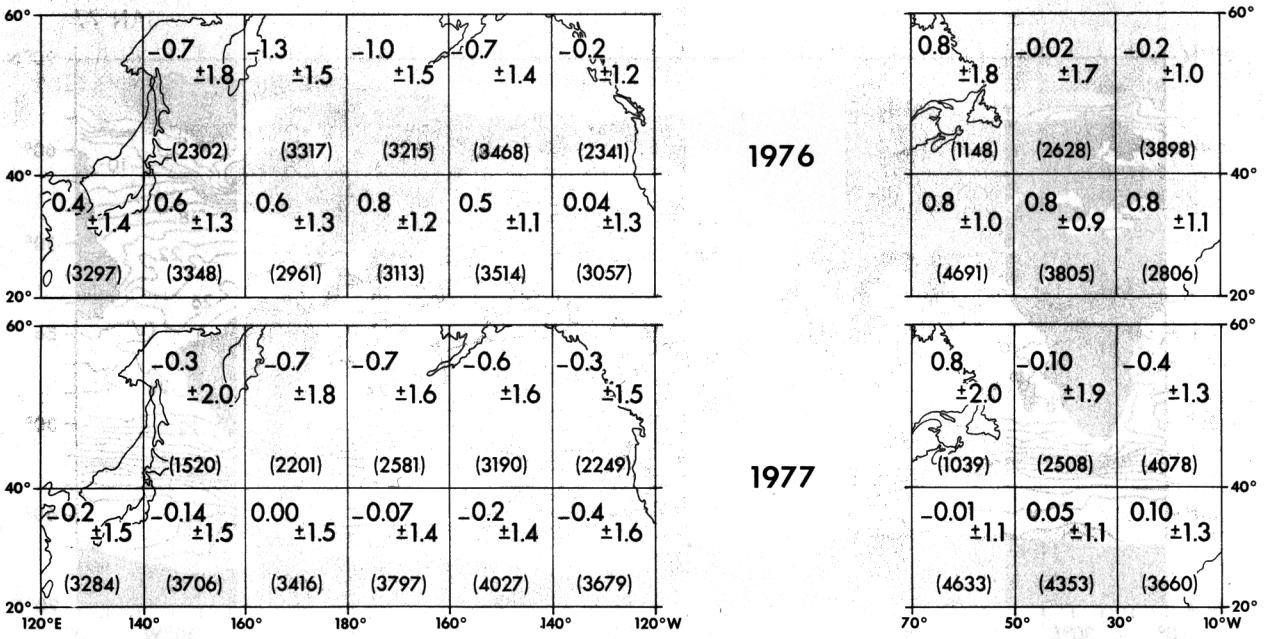

Fig. 7. The mean difference and the standard deviations of the difference between the satellite and ship SST for the Pacific Ocean and the Atlantic Ocean in (top) 1976 and (bottom) 1977. The geography is shown to indicate the locations. For example, in 1976, in the area south of the Aleutian Islands, i.e., 180°W–160°W and 60°N–40°N, the mean difference is −1.0 and the standard deviation is ±1.5, where the sample number of the pair of SST data used is 3215.

Figure 7 shows the statistics over the domains of the North Pacific (20°–60°N, 120°–E–120°W) and the North Atlantic (20°–60°N, 70°W–10°W) for the annual averages of 1976 and 1977 separately. The numbers shown are mean differences, standard deviations, and sample numbers, in parentheses. In April 1977 a new method to detect clouds and improve the atmospheric attenuation correction was introduced into the satellite retrievals. This resulted in a reduction of the sample size and supposedly improved the quality of the data. Using Table 1 and Figure 7 we do indeed notice that the mean differences are reduced after the new correction, but the standard deviations are increased. The mean differences, shown in Figure 7, range from −1.3°C to +0.8°C, and the standard deviation ranges from ±0.9° to 2.0°, with ±1.43°C being the arithmetic average for the entire period and domain. It is interesting to note that the standard deviation is particularly large in the subarctic regions such as the Sea of Okhotsk and the western Atlantic near Nova Scotia, where the SST behavior is known to be capricious owing to the violent convective overturning and the intermittent formation of warm surface water.

In these comparisons, both data sources exhibited a large

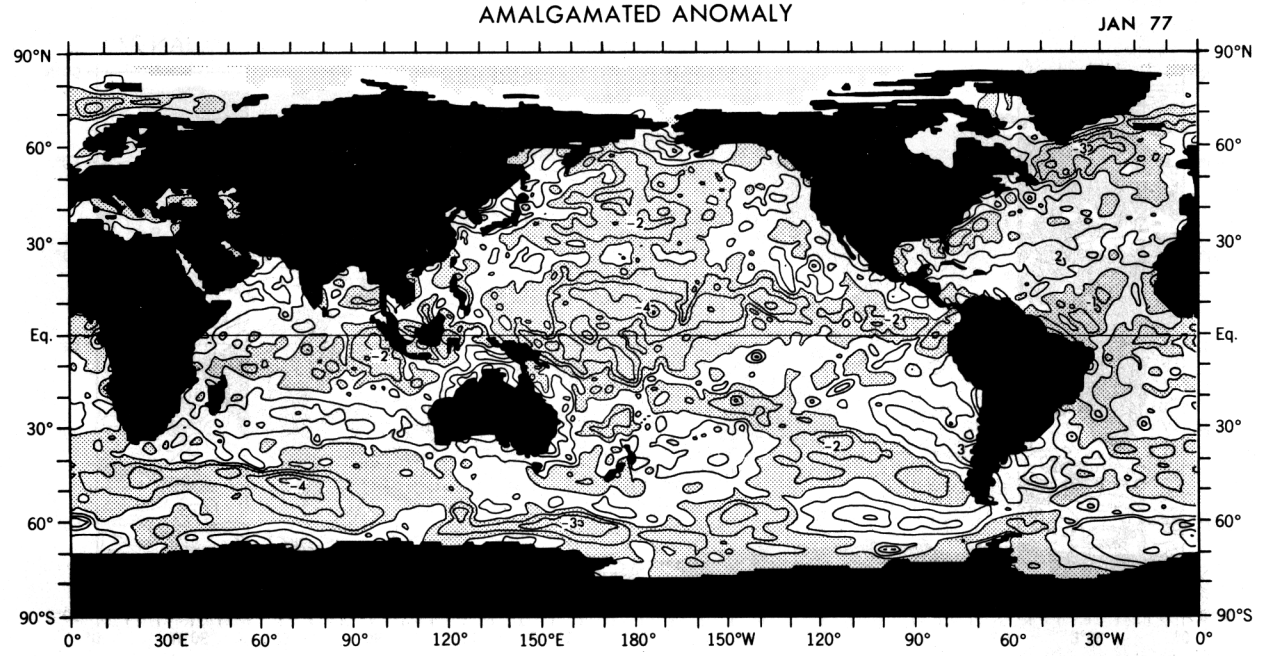

Fig. 8. The amalgamated SST anomaly (°C) for January 1977. The negative anomalies are shaded.

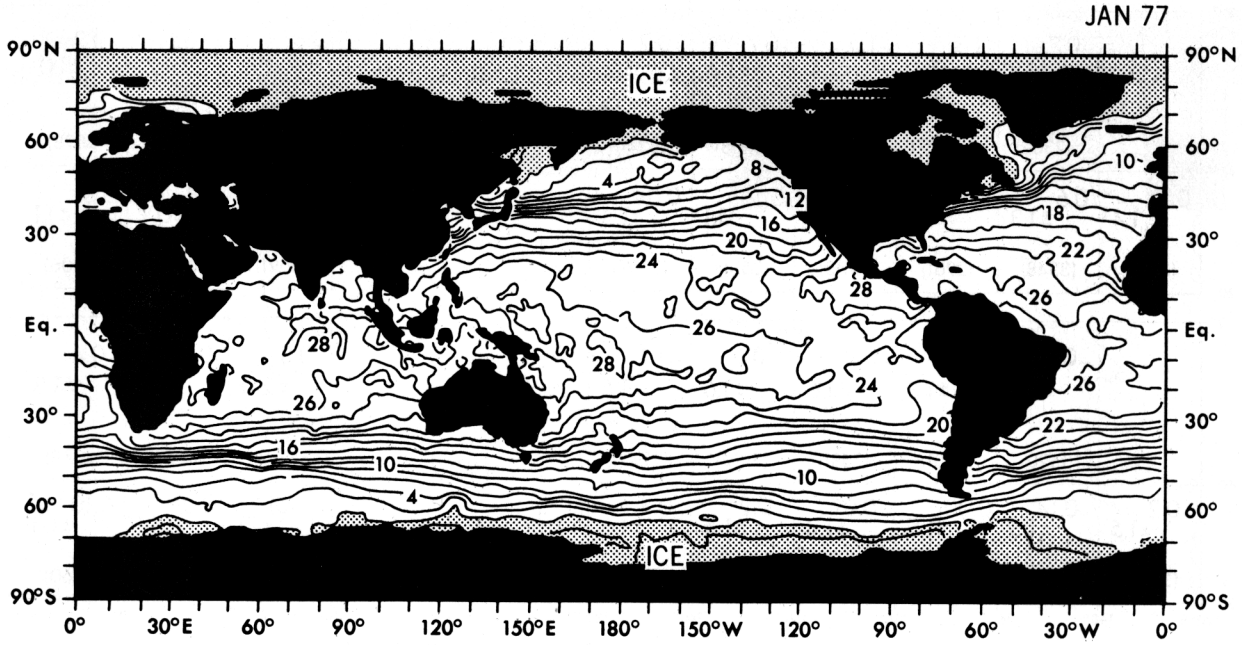

Fig. 9. The total SST (°C) based on the amalgamated anomaly for January 1977 in Figure 8. The ice covers are shaded.

error. As *Tabata* [1978*a*] mentioned, in his comparison of merchant ship SST's with SST's from station P and fixed NOAA buoys, the standard deviation on the average was ±1.5°C. It would have been ideal to compare satellite data with a more reliable observing system such as the NORPAX data, but then an overall view of the geographical distribution of the discrepancy could not have been obtained.

4. Analysis Maps: Level III Data

Using the spatially inhomogeneous distribution of level II SST data, an analysis was made to a regular grid; the resulting data are called level III data. The method of the analysis was adapted from that of *Levitus and Oort* [1977], who used this technique to produce a climatological oceanic analysis for the whole depth of the ocean based on data from research vessels. The method is the classical 'objective' analysis technique, using an iterative difference-correction scheme, i.e., the combination of Bergthörsson-Döös and Cressman [see *Gandin*, 1963]. The first guess field is given, and the analysis is successively refined by including the effects of observation data. The correction procedure at a gridpoint value is computed as a distance weighted average of all the residuals, the difference of guess values from observations, that lie within an area around the gridpoint defined by the influence radius. The weighting function is

$$w = \begin{cases} \exp(-4r^2/R^2) & \text{for } r \le R \\ 0 & \text{for } r < R \end{cases}$$

where r is the distance of an observation from the gridpoint and R is the influence radius.

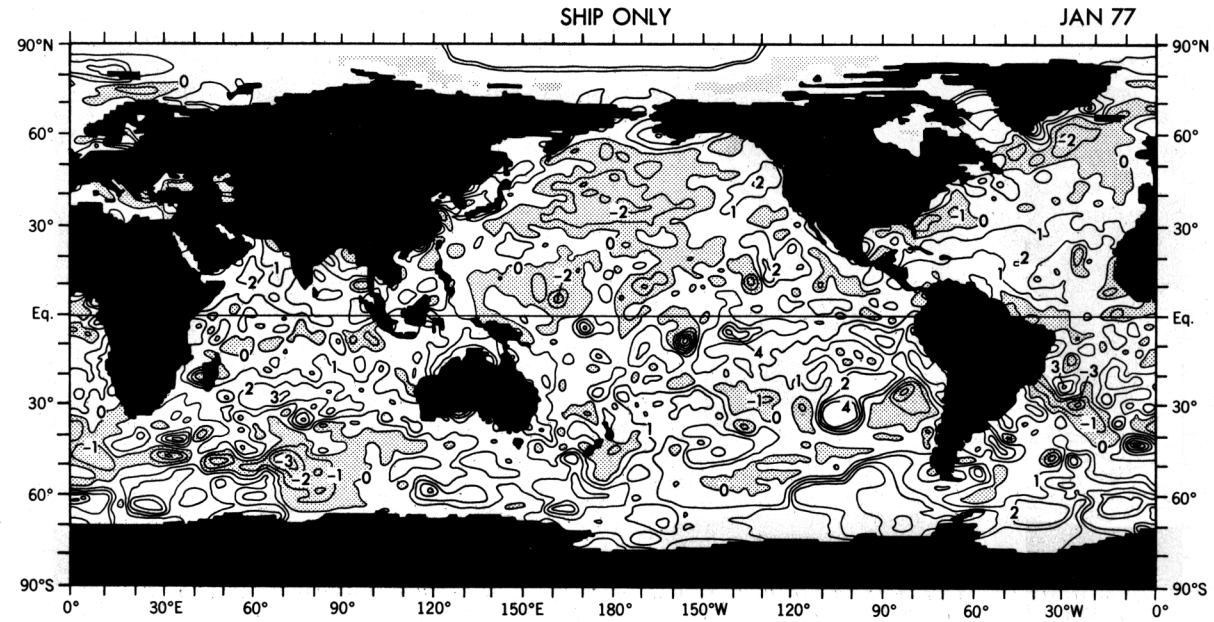

Fig. 10. The SST anomaly (°C) based on the ship data only for January 1977.

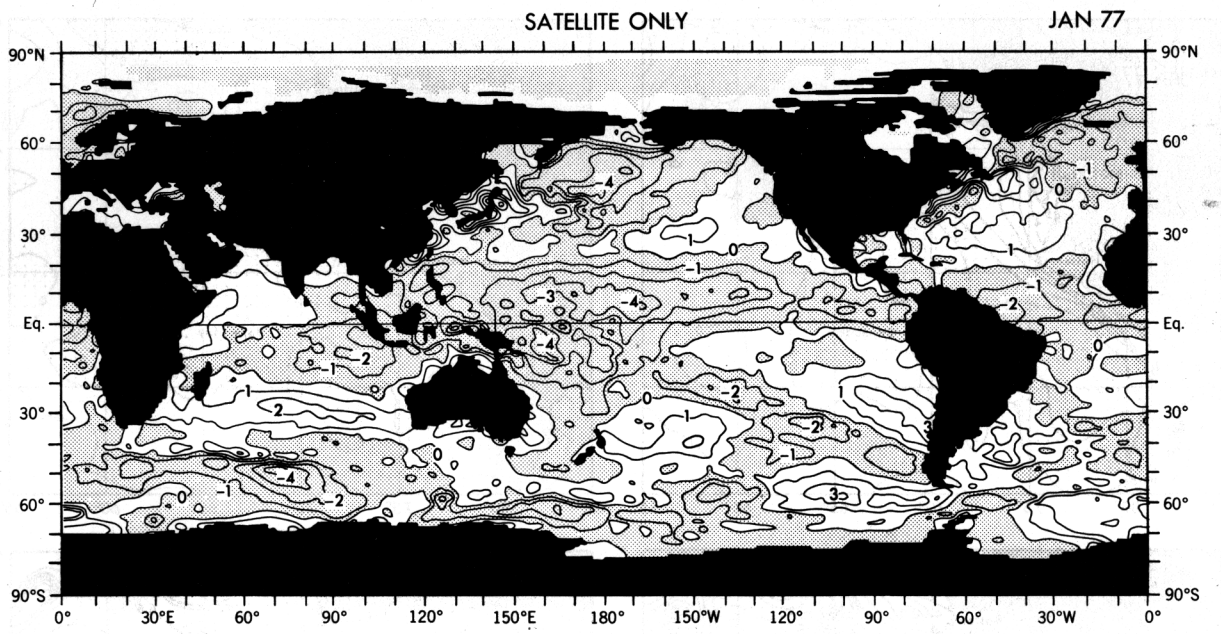

Fig. 11. The SST anomaly (°C) based on the satellite data only for January 1977.

In adapting their analysis scheme we applied the following specifications:

1. The first guess field was the climatological monthly SST, taken from RAND [*Alexander and Mobley,* 1976]. We understand that these normals of RAND are the merged products of NCAR [*Washington and Thiel,* 1970] and FNWC.

2. Sea-ice limits were taken from RAND normals for every month, since for any individual month the data were not readily available, even from satellites.

3. Several iterations were performed by using the analysis produced in each iteration as the guess field for the next iteration. In the procedure we started with a large influence radius and then successively decreased the radius so as to capture smaller scale features.

4. For the first iteration of the analysis, only satellite

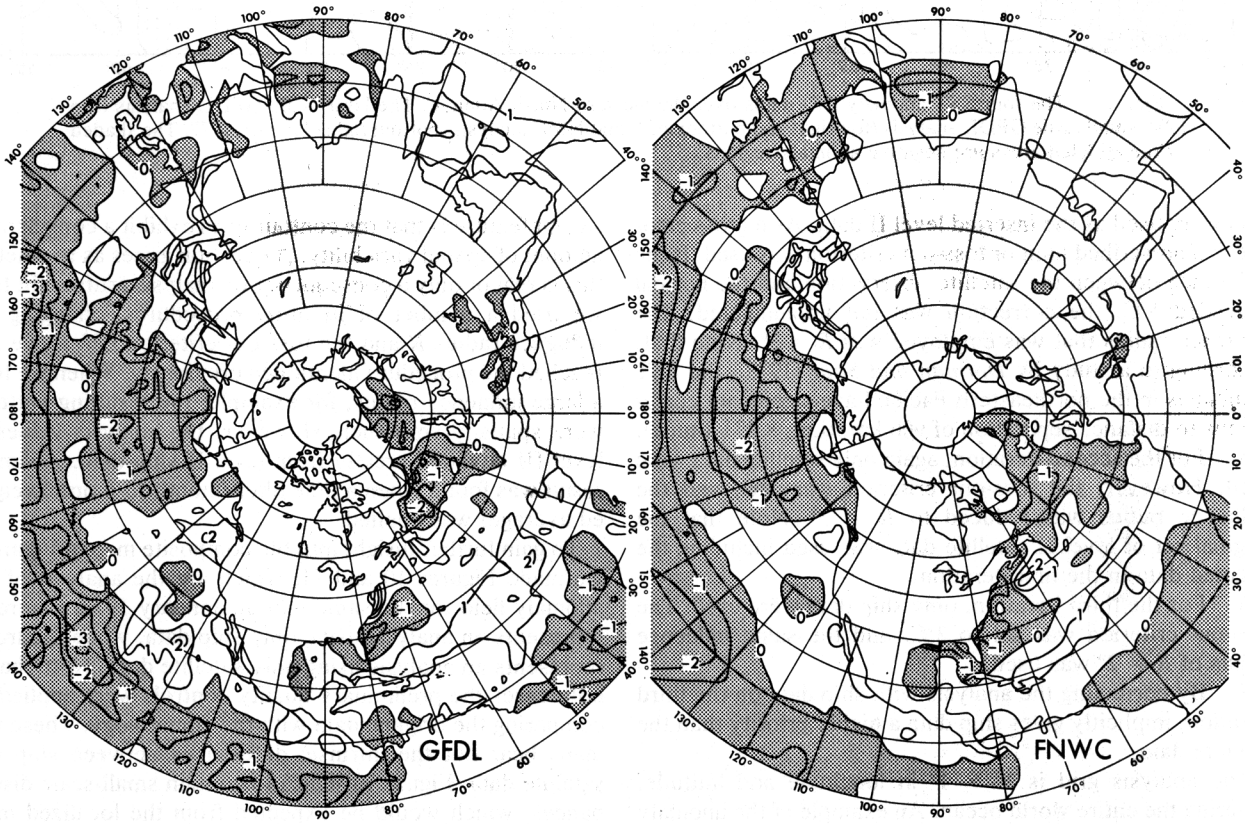

Fig. 12. The comparative display of the GFDL and the FNWC analysis of SST anomaly (°C) over the northern hemisphere for January 1977. The areas of negative anomaly are shaded.

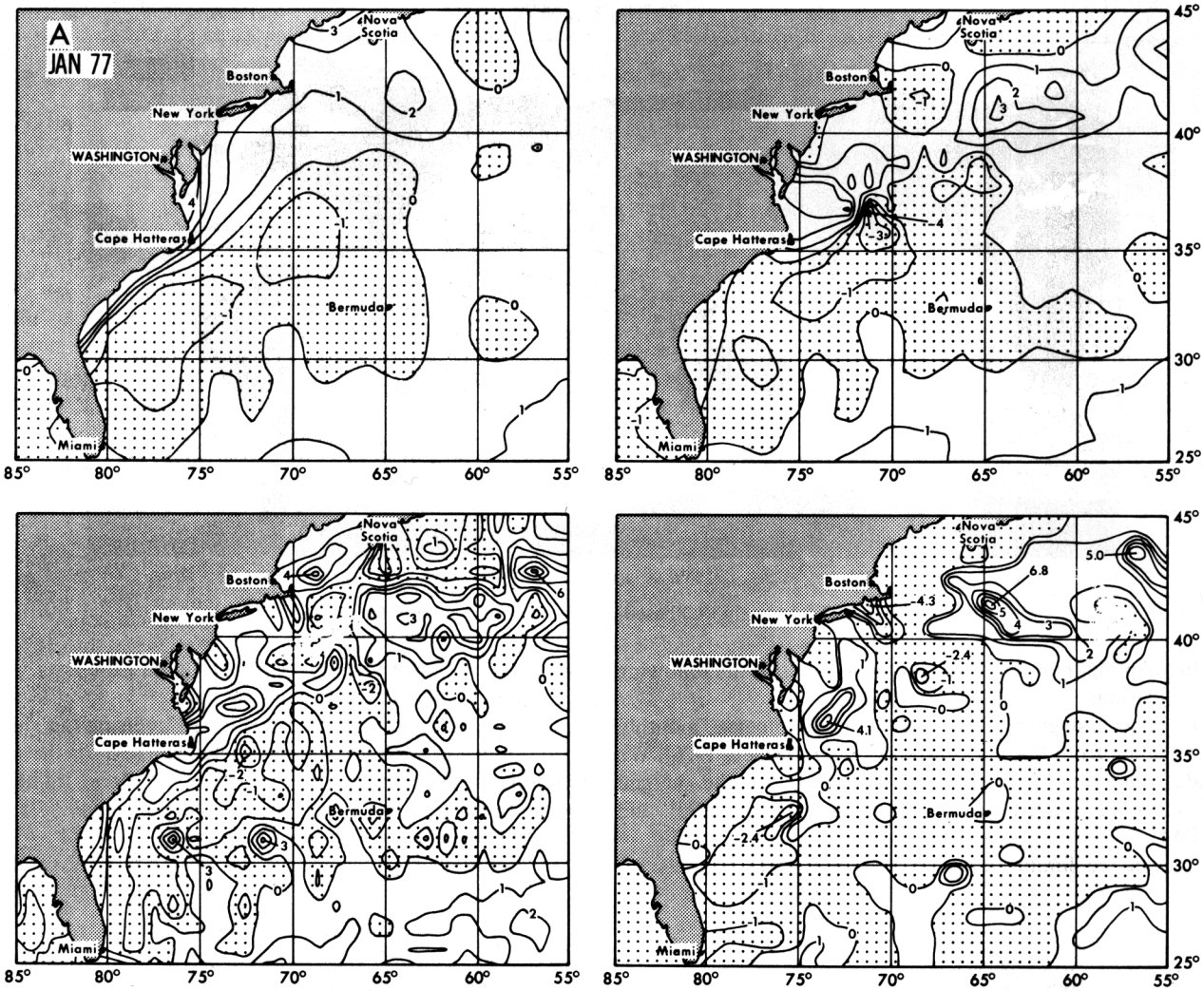

Fig. 13. The four SST anomaly (°C) maps over the western North Atlantic. The large-scale GFDL analysis (top left), small-scale GFDL analysis (top right and bottom left), and NMC analysis (bottom right) January 1977. The shaded or the stippled areas are negative anomaly regions.

data were used as the inserted level II data. As a gross error check a prescribed limit or toss-out criterion was used. If the difference between the satellite observation and the normal exceeded 5°C, the correction was not implemented. The influence radius that was employed was $R = 3°$. Note that, according to a study by *Dorman and Saur* [1978], the SST anomalies in the northeastern Pacific have significant correlations to distance separation of 900 km, (i.e., 8.2° latitude).

5. For the second iteration, again only satellite data were used. However, the toss-out criterion was 3°C, and the influence radius was reduced to $R = 2°$. Note that the original set of level II satellite data was used including the rejected data in the first iteration.

6. For the third iteration, only ship data were used. The toss-out criterion was set to 3°C, and the same influence radius of $R = 2°$ was used.

7. By correcting the analysis with ship data on the third iteration, implicitly gives ship data a higher priority than the satellite data.

The analysis grid is 1° × 1° in longitude and latitude, covering the entire world ocean. An example of the anomaly map for January 1977 is displayed in Figure 8, and the total SST map for the same month is in Figure 9. Perhaps the salient feature is that the contour lines exhibit a considerable amount of spatial variability. A question arises as to whether this is real or only a consequence of analysis artifact. In fact, we tried a number of iteration procedures, changing the influence radius R and the toss-out criterion before we had reached the procedure mentioned previously. When we took a large influence radius, for example, the resulting patterns were spatially smoother. However, the analysis values of level III deviated greatly from level II ship data. A similar result was found when a time filter (month-to-month weighted average) was applied.

To gain further insight into the composite map in Figure 8, we made Figures 10 and 11, which are the analysis of the anomaly field for the same month, January 1977. Figure 10 represents an analysis using only ship data, while Figure 11 represents an analysis using only satellite data. Note that in both cases the preliminary quality controls were applied by comparing the original data with the climatology. These two maps bear out the intrinsic differences between ship and satellite data. Figure 10 seems to contain small-scale disturbances, which would be expected from the localized measurements of ships. Recalling Figure 2 one can see that the southern hemisphere ship analysis is not very creditable. In

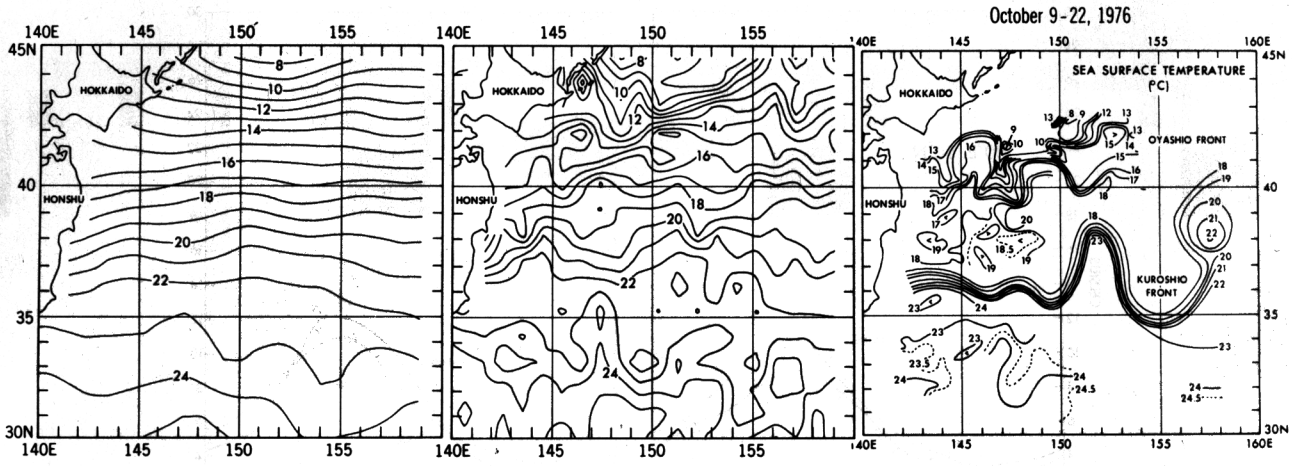

Fig. 14. The three total SST (°C) maps over the western North Pacific. The (left) large-scale GFDL analysis, (middle) the small-scale GFDL analysis, both of which are the monthly mean maps for October 1976, and (right) *Cheney*'s [1977] map for October 9–22, 1976.

Figure 11 the patterns seem to be spatially smoother, which is also expected due to the area averaged measurements of satellite. We also note the increased amplitudes for spatially large-scale patterns in the satellite analysis.

The difficulty in the production of level III SST data is the quality control, choosing limits of toss-out criteria, of level II data. It is extremely difficult to decide whether a particular datum is erroneous or not. Even if the datum is true, the spatial representativeness is a problem. For this reason we may have discarded true data excessively in our level III data. A justification is, however, that our interest is in the large-scale patterns of SST anomalies; and, for that objective, isolated small-scale feature may not be important.

5. Comparison of Level III Data

Throughout this section, the GFDL analysis that is referred to is the amalgamated ship and satellite analysis.

Three kinds of comparisons are shown in this section.

1. Figure 12 is the SST anomaly maps of the FNWC [see *Wolff et al.*, 1965; *Holl et al.*, 1971] and GFDL for January 1977 on a stereographic projection map. Overall, there is fair agreement between FNWC and GFDL. A detailed look reveals, however, that the GFDL map includes more small-scale features, whereas the map of FNWC is characterized by a smoother pattern. It should be noted that FNWC uses climatology in data sparse regions, thus accounting for the smooth pattern. A large difference is found off the west coast of the United States; GFDL has +2.1°C, whereas FNWC has +0.8°C. Although not shown here, we also compared the GFDL analysis with the NESS analysis. It is appreciably different from both GFDL and FNWC. The NESS map did not include ship data. We also made a comparison with SIO analysis (not shown here). The anomaly patterns are similar; however, the SIO maps are smoother and colder by about 1°C. Other months during the period of 1976 and 1977 were also compared in a similar fashion, and it appears that in general the same conclusion holds.

It is common, however, in the four analyses of January 1977 that the extensive area of the negative anomalies is located in the central North Pacific, with its minimum at 160°E–180°W, and 40°–50°N. This is the important feature, as was mentioned in the 'Introduction.' This cold anomaly might be crucial to the subsequent abnormal atmospheric temperatures over the United States. The minimum value of the SST anomaly in both the GFDL and the FNWC maps is about −2.5°C. On the other hand, in the NESS analysis, the value is a little less than −6°C, and our analysis using the satellite data alone in Figure 11 was less than −4°C. These very cold anomalies may be due to poor cloud correction algorithms. It should be noted that these comparisons are made in the northern hemisphere where ship data is common to all analysis. We do not have a southern hemispheric comparison since no analysis was available; however, our southern hemisphere analysis primarily reflects satellite data, and as was previously noted in regions of persistent cloudiness (45°S to pole) the analysis is suspect.

2. The second comparison is made with the analysis of National Weather Service's National Meteorological Center (NMC) [*National Weather Service*, 1977] for the western North Atlantic off the east coast of the United States. This area is a domain of dense data coverage by conventional observations and of high variability of ocean temperature due to the meandering Gulf Stream and the confluence of the cold Labrador Current with the warm Gulf Stream. This region is also noted for the enormous heat exchange between the ocean and the atmosphere [*Budkyo*, 1963; *Bunker and Worthington*, 1976].

Figure 13 includes the SST anomaly maps for January 1977. There are four different types of maps (i.e., the large-scale analysis of GFDL (top left), the small-scale analysis of GFDL (top right and bottom left), and the NMC analysis (bottom right)). The large-scale analysis of GFDL is exactly the same as the anomaly map shown in Figure 8 and was extracted from it. In this section we will be only concerned with the two maps (i.e., the top left and the bottom right); the other two (the small-scale analysis) will be discussed in a later section.

The NMC analysis was based on not only data from ships of opportunity but also on a number of research ships that were exchanged on the Global Telecommunications System under the IGOSS (Integrated Global Ocean Station System) program. They did not include satellite data, except in locating the Gulf Stream axis and the mesoscale eddies. It is typical of this type of analysis that data indicating many warm 'eddies' (rings) show up and that scattered about are a number of isolated temperature anomalies above 5°C. For

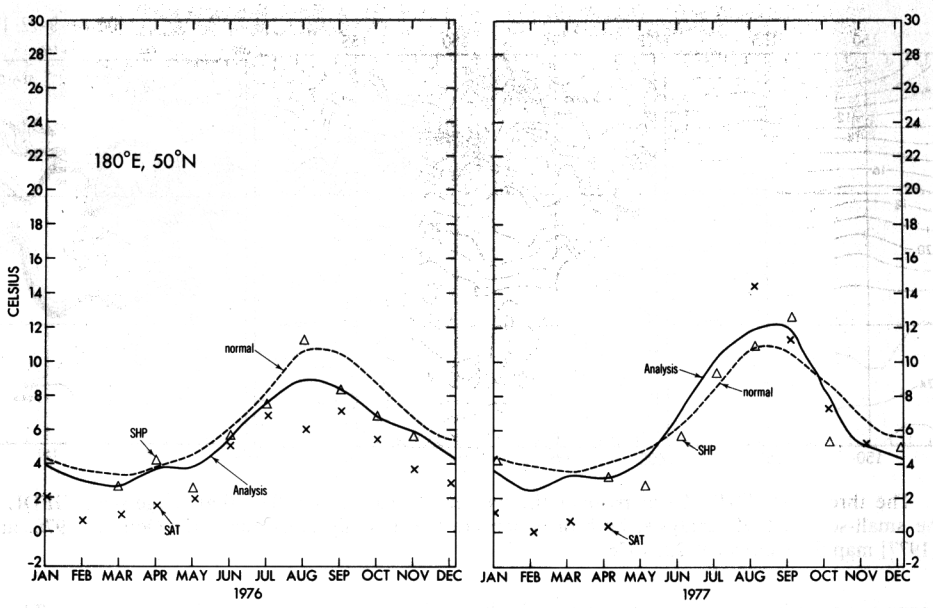

Fig. 15*a*

Fig. 15. The total SST for 2 years of 1976 and 1977 at five points over the North Pacific. The solid lines are the analysis (large scale); the ship data and the satellite data are marked by triangles and crosses, respectively; and the dashed lines are the climatological normals.

example, a +6.8°C anomaly is located south of Nova Scotia. Note that for this anlaysis only 1° quadrangles containing at least four observations were used.

The GFDL large-scale analyses, on the other hand, does not include these 'eddies.' Yet the overall features resemble those of NMC analysis. The overall trends are common to both analysis for other months as well.

3. The third comparison was made against a hand analysis of *Cheney* [1977]; that is, the synthesis of the SST data during October 9–22, 1976. This anlaysis off the coast of Japan is in an area of strong surface temperature gradients and the confluence region of the cold Oyashio with the warm Kuroshio Currents.

Figure 14 includes Cheney's analysis (right) as well as GFDL's large-scale (left) and small-scale analysis (middle). GFDL's large-scale analysis is exactly the same as in Figure 8. The GFDL map is a monthly mean SST for October 1976, and, therefore, it is different from Cheney's in the averaging time length. In this section again, we will be only concerned with the left and the right panels; the middle one will be discussed later.

Cheney [1977] used data of numerous flight measurements, supplemented by research ship data. Particularly the airborne expendable bathythermograph and airborne radiation thermometer were used to track the Kuroshio. The right-hand panel of Figure 14 reveals two oceanic fronts, that

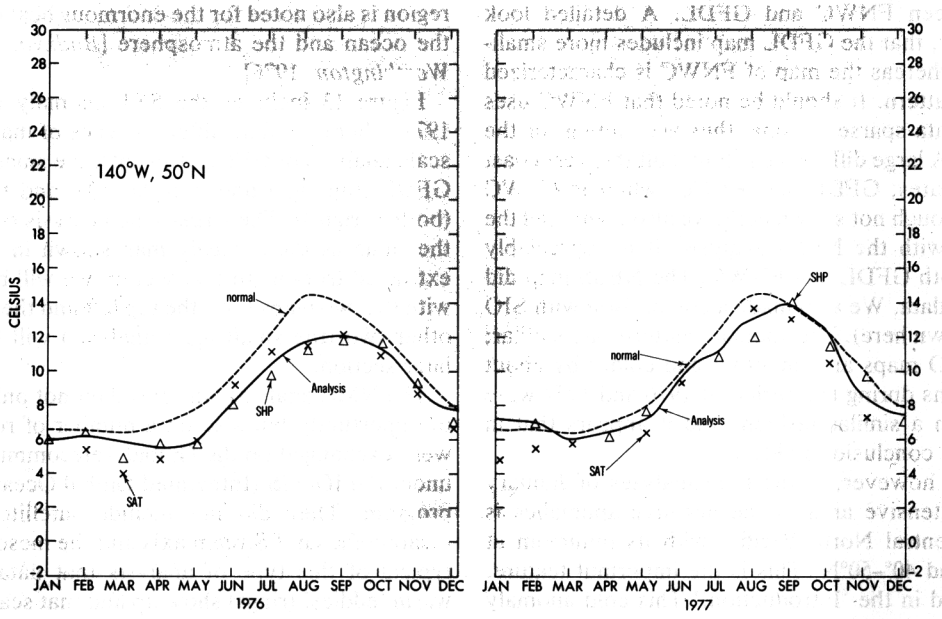

Fig. 15*b*

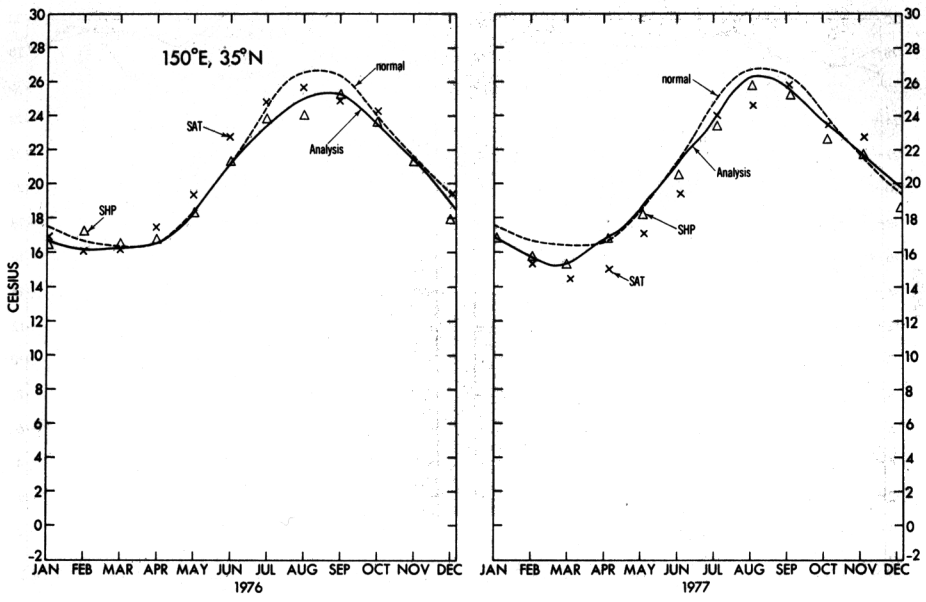

Fig. 15*c*

is, Oyashio and Kuroshio fronts [*Uda,* 1963; *Roden,* 1972] and two anticyclonic gyres. On the other hand, the GFDL analysis (left) does not resolve any of these fronts and eddies; in fact the contour lines appear quite smooth.

6. VARIABILITIES

Taking five sample points over the Pacific Ocean we show the time series of the analyzed SST for 1976 and 1977 in Figure 15. The values are the 1° quadrangle SST around (180°E, 50°N), (140°W, 50°N), (150°E, 35°N), (140°W, 35°N), and (180°E, 0°). The climate normals are shown by dashed lines, and the ship and satellite data are also plotted separately whenever they were available.

In contrast to the space variabilities, the time evolution curves are very smooth in spite of the fact that we did not apply any time smoothing or filtering. It may be noticed that the amalgamated analysis curves are closer to the ship data points; this is because, as mentioned previously, our final analysis pass uses ship data to correct. Even though the influence radius in the analysis was small, neighboring points would modify a point so that it would deviate from observations. Unfortunately, the uncertainty in ship/satellite data and analysis technique is as large or larger than the anomalies we wish to study.

The latitudinal distributions of SST variance as revealed in our analysis are displayed in Figures 16 and 17 for the Pacific and Atlantic oceans. The curves are the root-mean-square of the SST anomaly, and were calculated from

$$[\overline{(T - T_n)^2}^{\lambda}]^{1/2}$$

where T is the amalgamated SST, T_n is the climatic normal of SST for January, and $\overline{(\quad)}^{\lambda}$ is the zonal average over the respective ocean basin. Both figures include three Januaries,

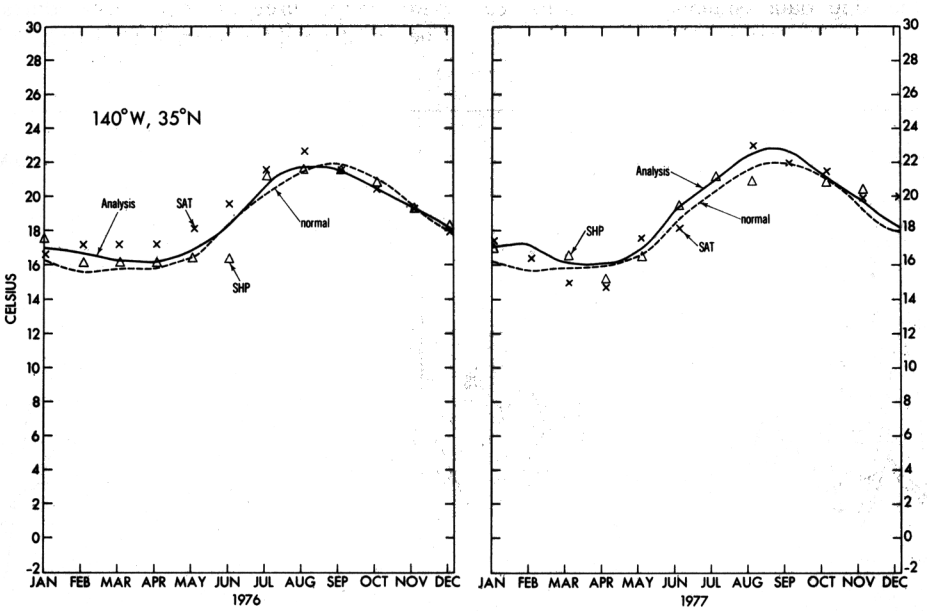

Fig. 15*d*

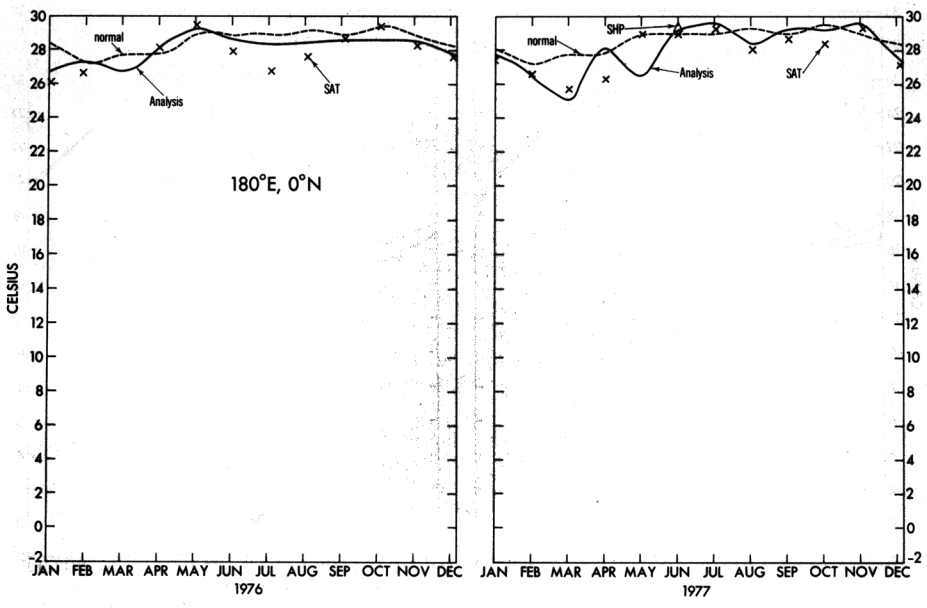

Fig. 15*e*

1976, 1977, and 1978. According to these figures, the variability of the anomaly is highest, 2.3°C, at the zone of 35°–70°S in the southern hemisphere and 2.2°C at the subarctic zone of 70°N in the northern hemisphere. At the equatorial region, this variability is somewhat smaller, say 0.6°C over the Atlantic Ocean and 1.5°C over the Pacific Ocean.

Attempting to place the above and the preceding sections into climatological perspective, we have a list on the order of magnitudes for each component of the SST variabilities. From the larger to the smaller components, they are the latitudinal difference between the equator and polar regions, ~ 28°C; the seasonal difference between the maximum and the minimum (for example, March and August at 30° ~ 60°N over the Pacific Ocean), ~ 10.5°C; the variability of anomalies of the small scale eddies off the east coast of the United States (root-mean-square), ~ 3.2°; the variability of large-scale anomalies (root-mean-square): northern hemisphere, ~ 1.0°, southern hemisphere, ~ 1.5°; the difference between the satellite and the ship data (standard deviation, see section 3), ~ 1.4°.

7. SMALL-SCALE ANALYSIS

Finally, a test on the fine thermal structure analysis will be mentioned. To enhance the small-scale variance of the SST in the analysis map, we specified different toss-out criteria and radii of influence in the Levitus-Oort analysis program. The toss-out criteria in the large-scale analysis in section 4 may be represented by (5°, 3°, 3°C) for the first, second, and third iteration, and the radii of influence were 3°, 2°, 2°. On the other hand, in the first new small-scale analysis, the toss-out criteria were 5°, 3°, 3°, and the radius of influence were 1°, 1°, 1°. In the second small-scale analysis, the toss-out criteria were 5°, 7°, 5°, and the radii of influence were 1°, 1°, 1°.

Figure 13 (top right and bottom left) is the result of a test for the North Atlantic east of the United States, which is to be compared with the other maps in Figure 13. In January 1977, negative anomalies dominated in this region. In the NMC map, three distinct warm eddies were located in Chesapeake bight, centered at +4.1°C; 74°W, 36°N, off Nova

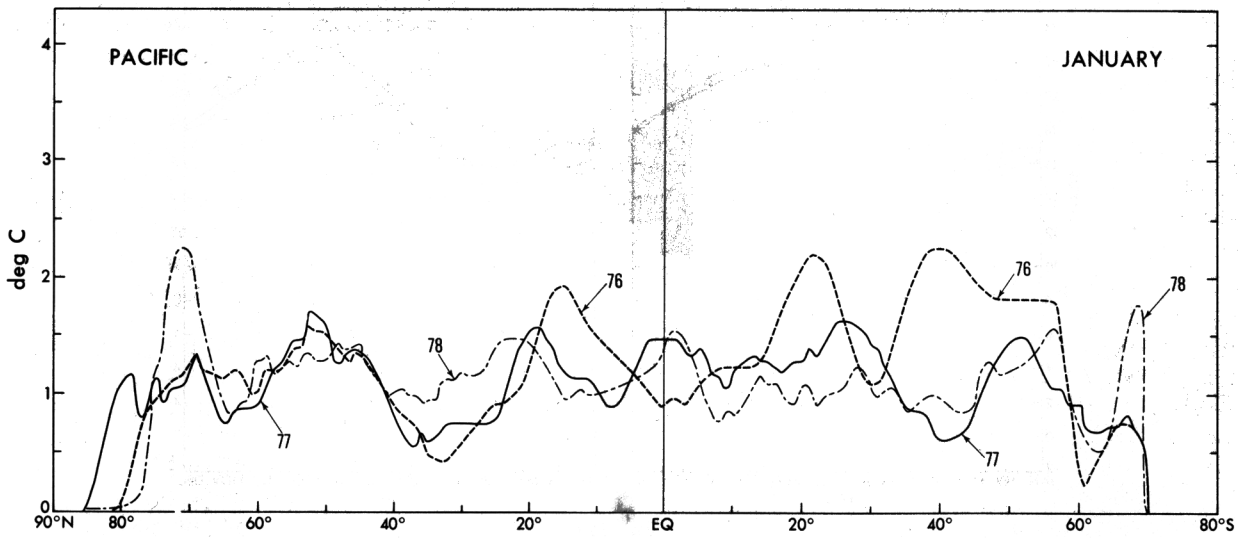

Fig. 16. The variance of the SST anomalies for three Januaries (1976, 1977, and 1978) for the Pacific Ocean.

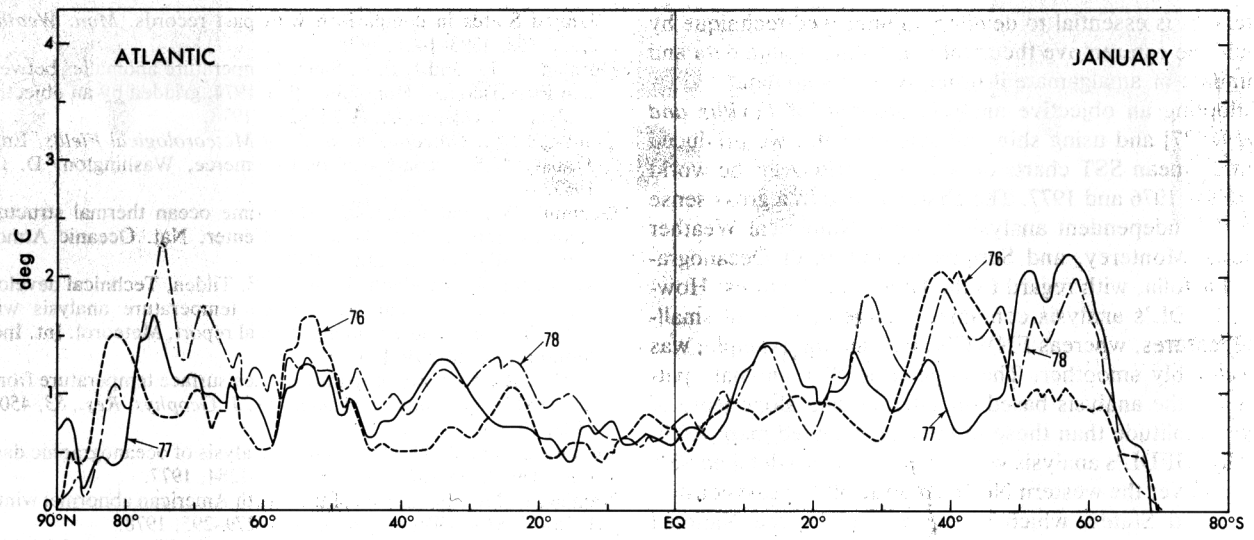

Fig. 17. The same as in Figure 16 but for the Atlantic Ocean.

Scotia (+6.8°C; 65°W, 41°N), and in the northeastern corner of the panel (+5.0°C; 57°W, 44°N). Corresponding to those, three positive anomalies are also seen in the GFDL small-scale analysis (bottom left); the intensities are +4.2°C, +3.2°C, and +5.1°C. It is, however, annoying that in the GFDL small-scale analysis (bottom left) the seemingly erroneous spots, for example, at 75°W, 31°N and 72°W, 31°N in January are now contained. These spots have crept in due to the relaxed toss-out process. The small-scale analysis in the bottom right is, therefore, a compromise.

Summarizing the above, one may say that the eddies in the GFDL maps are now more noticeable and resemblance of the GFDL small-scale analysis to the NMC analysis has been increased. Particularly the warm eddies along the coastlines of Maryland, Delaware, and New Jersey have become pronounced. Yet the data quality control presents an even more formidable problem; the identification of whether certain features are eddies or errors is indeed difficult.

Figure 14 (middle) is the small-scale analysis for the North Pacific east of Japan in October 1976, based on the second new specification for quality control and the radius of influence. The new analysis looks quite different from the previous smoothed pattern (left), and the temperature gradient between 36°N and 44°N has been appreciably increased. However, the meander of the Kuroshio current and the fronts were not well produced. In Cheney's chart, two well-defined fronts associated with the subarctic-subtropical transition zone are found, there exists a vast isothermal region between them, and three pronounced anticyclonic gyres exist. In GFDL's analysis, however, these features may be or may not be included; anyway, the similarity is not good. In this case also, quality control of the data appears to be very important. In our case, the ship level II data were provided at 1° quadrangles, but, ideally, a more elaborate 'buddy' check would have been necessary for defining the 1° quadrangle data.

It is questionable whether satellite data may be used to identify eddies and fronts. The satellite data we used in this study does not seem adequate for this purpose, perhaps because the data were on too broad a scale. But, since the satellite imagery of the ocean surface has revealed the capability of resolving subtle thermal variation, it may be reasonable to think that the digitized infrared data would have the equivalent capability, if the space resolution is sufficiently fine. In fact, *Roden and Paskansky* [1978] examined the feasibility of estimating rates of frontogenesis and frontolysis, using satellite SST in 1977 [*National Environmental Satellite Service,* 1977], and found a reasonable agreement between the computed and observed patterns in subtropical latitudes east of 175°E, and *Legeckis* [1978] mentioned that improvements in the satellite infrared scanner has allowed the description of fronts at the surface of the ocean in considerable detail.

Finally, another point may be added. For the production of the atmospheric level III data, GFDL has been using successfully the Optimum Interpolation Analysis method [see *Gandin,* 1963]. The technique is designed to achieve statistically the minimum root-mean-square error from the observation and is advantageous to select adequate analysis parameters based on the reliability of observations. To implement this method for the SST analysis, statistical information on the covariance of observations is required, which needs an extensive preparatory study [*Dorman and Saur,* 1978; *Bretherton et al.,* 1976].

8. Conclusions and Remarks

Using monthly mean SST data derived from NOAA-5 soundings, the quality of satellite data was examined relative to the observations of ships of opportunity. The standard deviation of the difference between the satellite and ship data was about ±1.4°C (the sampling error was not removed), which is not small in view of the magnitudes of the anomalies we study. Any systematic seasonal variation in the satellite data deviation was hardly detectable, and the supposed improvement of the data quality from 1976 to 1977 was discernible but not large. The difference between the two data sources was particularly large in the subarctic regions such as the Sea of Okhotsk and Baffin Bay areas.

We understand that the quality of the satellite retrievals and the data processing techniques are still under continuing development. In years to come we have to rely on satellite data over a wide area of the ocean. Yet there is a fundamental difference between the satellite and the ship observations; one is an area averaged skin temperature, while the other is an engine intake temperature for a point at a depth of 3 ~ 6

meters. It is essential to develop an improved technique by which one can remove the areal bias from satellite data and assimilate or amalgamate it properly with ship data.

Adopting an objective analysis program of *Levitus and Oort* [1977] and using ship and satellite data, we produced monthly mean SST charts on a 1° × 1° grid over the world ocean for 1976 and 1977. The charts agreed in a gross sense with the independent analysis at Fleet Numerical Weather Central, Monterey, and Scripps Institution of Oceanography, La Jolla, with regard to the large-scale features. However, GFDL's analysis contained a large number of small-scale features, whereas FNWC's analysis, for example, was considerably smoother. The large-scale SST anomaly patterns for the analysis based on satellite data alone were of larger amplitude than those in the amalgamated map. Additionally, GFDL's analysis was compared with a detailed SST analysis over the western North Atlantic off the east coast of the United States, which was produced by the National Weather Service, Washington, D.C., and also an analysis by *Cheney* [1977] over the Oyashio and Kuroshio fronts off the coast of Japan. These comparisons revealed that even GFDL's analysis failed to reproduce small-scale features due to oceanic mesoscale eddies and fronts. By relaxing the toss-out criterion for ship observations and by using a smaller domain of data influence in the analysis, one can show that the SST maps become relatively closer to the others. It appears, however, that quality control of the data is very important for the analysis, particularly with regard to whether a datum is the reflection of an eddy or of an error. It is hoped that fine resolution satellite data will add some insight in this regard.

Acknowledgments. The authors gratefully acknowledge the cooperation and suggestions of D. McLain, S. Levitus, A. Oort, and R. Dickson. Thanks also go to E. Barker, D. Cayan, C. K. Stidd, M. Tsuchiya, B. Pichel, and J. Namias for providing valuable suggestions and/or reading the manuscript.

REFERENCES

Alexander, R. C., and R. I. Mobley, Monthly average sea-surface temperature and ice-pack limits on a 1° global grid, *Mon. Weather Rev., 104,* 143–148, 1976.

Barnett, T. P., W. C. Patzert, S. C. Webb, and B. R. Bean, Climatological usefulness of satellite determined sea-surface temperatures in the tropical Pacific, *Bull. Am. Meteorol. Soc., 60,* 197–205, 1979.

Bernstein, R., L. Breaker, and R. Whirtner, California current eddy formation: Ship, air and satellite results, *Science, 195,* 353–359, 1977.

Bretherton, F. P., E. Davis, and C. B. Fandry, A technique for objective analysis and design of oceanographic experiments applied to MODE-73, *Deep Sea Res., 23,* 559–582, 1976.

Brower, R. L., G. S. Gohrband, W. G. Pichel, T. L. Signore, and C. C. Walton, Satellite derived sea-surface temperatures from NOAA spacecraft, *Tech. Mem., NESS 79,* Nat. Oceanic Atmos. Admin., Washington, D.C., 1976.

Budyko, M. I., *Atlas of Heat Balance of the Earth,* Transl. from Russian, *WB/T-106,* U.S. Weather Bureau, Washington, D.C., 1963.

Bunker, A. F., and L. V. Worthington, Energy exchange charts of the North Atlantic Ocean, *Bull. Am. Meteorol. Soc. 57,* 670–678, 1976.

Cheney, R. E., Synoptic observations of the oceanic frontal system east of Japan, *J. Geophys. Res., 82,* 5459–5468, 1977.

Davis, R. E., Predictability of sea surface temperature and sea level pressure anomalies over the North Pacific Ocean, *J. Phys. Oceanogr., 6,* 249–266, 1976.

Diaz, H. F., and R. G. Quayle, The 1976–77 winter in the contiguous United States in comparison with past records, *Mon. Weather Rev., 106,* 1393–1421, 1978.

Dorman, C. E., and J. F. T. Saur, Temperature anomalies between San Francisco and Honolulu, 1966–1974, gridded by an objective analysis, *J. Oceanogr., 8,* 247–257, 1978.

Gandin, L. S., *Objective Analysis of Meteorological Fields,* Engl. Transl., U.S. Department of Commerce, Washington, D. C., 1963.

Gemmill, W., and S. Larson, Real time ocean thermal structure analysis, report, Nat. Meteorol. Center, Nat. Oceanic Atmos. Admin., Washington, D.C., 1979.

Holl, M. M., R. Mendenhall, and C. E. Tilden, Technical developments for operational sea surface temperature analysis with capability for satellite data input, final report, Meteorol. Int. Inc., Monterey, Calif., 1971.

Legeckis, R., A survey of worldwide sea surface temperature fronts detected by environmental satellites, *J. Geophys. Res., 83,* 4501–4522, 1978.

Levitus, S., and A. H. Oort, Global analysis of oceanographic data, *Bull. Am. Meteorol. Soc., 58,* 1270–1284, 1977.

Namias, J., Multiple causes of the North American abnormal winter 1976–77, *Mon. Weather Rev., 106,* 279–295, 1978.

National Environmental Satellite Service, weekly maps of GOSST-COMP sea surface temperature for the North Pacific, Ser. MN 135 E and MN 180, Washington, D. C., 1977.

National Weather Service, Gulfstream 1, 2, 3, report, Nat. Oceanic Atmos. Admin., Washington, D. C., 1977.

Rao, P. K., W. L. Smith, and R. Koffler, Global sea-surface temperature distribution determined from an environmental satellite, *Mon. Weather Rev., 100,* 10–14, 1972.

Roden, G. I., Temperature and salinity fronts at the boundaries of the subarctic-subtropical transition zone in the western Pacific, *J. Geophys. Res., 77,* 7175–7187, 1972.

Roden, G. I., and D. F. Paskansky, Estimation of rates of frontogenesis and frontolysis in the North Pacific Ocean using satellite and surface meteorological data from January 1977, *J. Geophys. Res., 83,* 4545–4550, 1978.

Saur, J. F. T., A study of the quality of sea water temperatures reported in logs of ships' weather observations, *J. Appl. Meteorol., 2,* 417–425, 1963.

Strong, A. E., and J. A. Pritchard, Regular monthly mean temperatures of Earth's Oceans from satellites, *Bull. Am. Meteorol. Soc., 61,* 553–559, 1980.

Stump, H. G., and R. V. Legeckis, Satellite observations of mesoscale eddy dynamics in the eastern Tropical Pacific Ocean, *J. Phys. Oceanogr., 7,* 648–658, 1977.

Tabata, S., Comparison of observations of sea surface temperatures at ocean station P and NOAA buoy stations and those made by merchant ships travelling in their vicinities, in the Northeast Pacific Ocean, *J. Appl. Meteorol., 17,* 374–385, 1978*a*.

Tabata, S., An evaluation of the quality of sea surface temperatures and salinities measured at station P and line P in the Northeast Pacific Ocean, *J. Phys. Oceanogr., 8,* 970–986, 1978*b*.

Uda, M., Oceanography of the subarctic Pacific Ocean, *J. Fish. Res. Bd. Canada, 20,* 119–179, 1963.

Wagner, A. J., Weather and circulation of January 1977: The coldest month on record in the Ohio Valley, *Mon. Weather Rev., 105,* 553–560, 1977.

Walton, C. C., R. L. Brower, and T. L. Signore, Satellite derived sea surface temperatures by multi-channel regression, paper presented at Proceedings of the Symposium on Meteorological Observations from Space: Their Contribution to the First GARP Global Experiment, Committee on Space Research (COSPAR) of the International Council of Scientific Unions, Boulder, Colo., June 1976.

Washington, W. M., and L. G. Thiel, Digitized global monthly mean ocean surface temperatures, *NCAR-TN-54,* Nat. Center for Atmos. Res., Boulder, Colo., 1970.

Wolff, P. M., L. P. Carstensen, and T. Laevastu, Analysis and forecasting of sea surface temperature (SST), *Tech. Note. 8,* Fleet Numerical Weather Fac., Monterey, Calif., 1965.

(Received September 24, 1979;
revised April 1, 1982;
accepted April 5, 1982.)